

1 **Distribution of genetic diversity reveals colonization and philopatry of the loggerhead**  
2 **sea turtles across geographic scales**

3  
4 Baltazar-Soares Miguel<sup>1,2\*</sup>, Klein Juliana L.<sup>3\*</sup>, Correia Sandra M.<sup>4</sup>, Reischig Thomas<sup>5</sup>,  
5 Taxonera Amoros Albert<sup>6</sup>, Monteiro Roque Silvana<sup>7</sup>, Dos Passos Leno<sup>8</sup>, Durão Jandira<sup>9</sup>,  
6 Pina Lomba João<sup>10</sup>, Dinis Herculano<sup>11</sup>, Cameron Sahmorie J.K.<sup>1</sup>, Stiebens Victor A.<sup>1</sup>,  
7 Eizaguirre Christophe<sup>1,#</sup>

8  
9 Affiliations:

10 <sup>1</sup> School of Biological and Chemical Sciences, Queen Mary University of London, London, E1  
11 4NS, UK

12 <sup>2</sup> MARE-ISPA, Rua Jardim do Tabaco, 34, 1100-304 Lisboa Portugal

13 <sup>3</sup> Centre for Ecological Genomics and Wildlife Conservation, Department of Zoology  
14 University of Johannesburg, Auckland Park, South Africa

15 <sup>4</sup> Instituto do Mar (iMAr), Cova de Inglesa, C.P: 132 Mindelo, Sao Vicente, Cape Verde

16 <sup>5</sup> Turtle Foundation, An der Eiche 7a, 50678 Cologne, Germany

17 <sup>6</sup> Associação Projeto Biodiversidade, Mercado Municipal 22, Santa Maria 4111, Ilha do Sal,  
18 Cabo Verde

19 <sup>7</sup> Projeto Vitó Porto Novo. Porto Novo, Santo Antão Island, Cabo Verde.

20 <sup>8</sup> Foundation Maio Biodiversity, Cidade de Porto Inglês, Maio Island, Cabo Verde.

21 <sup>9</sup> Biosfera I, Rua de Moçambique 28, Mindelo, São Vicente, Cabo Verde

22 <sup>10</sup> Associação Ambiental Caretta Caretta. Achada Igreja, Pedra Badejo, Santa Cruz,  
23 Santiago, Cabo Verde

24 <sup>11</sup> Associação Projecto Vitó, Xaguete, São Felipe, Fogo, Cabo Verde.

25  
26  
27 \* These authors contributed equally to this study

28  
29 # To whom correspondence should be addressed: [c.eizaguirre@qmul.ac.uk](mailto:c.eizaguirre@qmul.ac.uk)

30  
31  
32  
33  
34  
35  
36  
37

38 **Abstract**

39

40 **Aim:** Understanding the processes that underlie the distribution of genetic diversity in  
41 endangered species is a goal of modern conservation biology. Specifically, how population  
42 structure affects genetic diversity and contributes to a species' adaptive potential remain  
43 elusive. The loggerhead sea turtle (*Caretta caretta*) faces multiple conservation challenges  
44 due to its migratory nature and philopatric behaviour.

45 **Locations:** Atlantic Ocean, Cabo Verde, island of Boavista

46 **Methods:** Here, using 4207 mtDNA sequences, we analysed the colonisation patterns and  
47 distribution of genetic diversity within a major ocean basin (the Atlantic), a regional rookery  
48 (Cabo Verde Archipelago) and a local island (Island of Boavista, Cabo Verde).

49 **Results:** Hypothesis-driven population genetic models suggest the colonization of the  
50 Atlantic has occurred in two distinct waves, each corresponding to major mtDNA lineages.  
51 We propose the oldest lineage entered the basin via the isthmus of Panama and sequentially  
52 established aggregations in Brazil, Cabo Verde and in the area of USA and Mexico. The  
53 second lineage entered the Atlantic via the Cape of Good Hope, establishing colonies in the  
54 Mediterranean Sea, and from then on, re-colonized the already existing rookeries of the  
55 Atlantic. At the Cabo Verde level, we reveal an asymmetric gene flow maintaining links  
56 across nesting groups despite significant genetic structure amongst nesting groups. This  
57 structure stems from female philopatric behaviour which could further be detected by weak  
58 but significant structure amongst beaches separated by only a few kilometres on the island of  
59 Boavista.

60 **Main conclusion:** To explore demographic processes at diverse geographic scales  
61 improves understanding the complex evolutionary history of highly migratory philopatric  
62 species. Unveiling the past facilitates the design of conservation programmes targeting the  
63 right management scale to maintain a species' adaptive potential and putative response to  
64 human-induced selection.

65

66

## 67 **Introduction**

68 The distribution of species is shaped by environmental variation acting both at macro and  
69 micro evolutionary scales (Ezard et al., 2011). Nowadays the distribution of biodiversity  
70 reflects specie's evolutionary history as well as eco-evolutionary dynamics within and across  
71 systems (Brunner et al., 2019). Because environmental factors (e.g. (Perry et al., 2005)) and  
72 past events of colonization (e.g. (Carotenuto et al., 2016)) leave genetic signatures,  
73 characterizing the distribution of genetic diversity sheds light on the mechanisms underlying  
74 the species and populations' distributions e.g. (Loveless & Hamrick, 1984; Ellegren & Galtier,  
75 2016). Understanding those mechanisms is crucial for the implementation of management  
76 and conservation measures to maintain species' adaptive potential (Frankham et al., 2002;  
77 Eizaguirre & Baltazar-Soares, 2014). The recent years have seen an increasing number of  
78 tools available to performed model-based inferences in evolutionary genetics (Csillery et al.,  
79 2010). Inferences are made over likelihood estimates of a certain set of pre-defined  
80 parameters constituting different evolutionary scenarios (Beaumont et al., 2010). Likelihood  
81 estimates can be obtained, for example, with exact calculations and usually use coalescent  
82 theory and Bayesian statistics to simulate phylogenies with Markov Chain Monte Carlo  
83 (MCMC) samplers (Drummond et al., 2005). Alternatively, likelihood estimates can be  
84 approximated with Approximate Bayesian Computation (ABC) mehtods which emmerged as  
85 an alternative that derives likelihood estimates through comparisons of summary statistics of  
86 simulated datasets and those obtained with observed data (Csillery et al., 2010). Being less  
87 demanding computationally, ABC facilitates hypothesis-testing to explain phylogeographic  
88 patterns that would be otherwise challenging to explore through computing exact likelihood  
89 estimates. For marine species, model-based inferences have contributed, for example, to  
90 understand oceanic divergence of humpback whales or the post glacial distribution of  
91 blacknose sharks (Jackson et al., 2014; Portnoy et al., 2014), revealing a promising tool to  
92 investigate the complex demographic patterns of philopatric and highly migratory species.  
93 Philopatry, the tendency of an organism to return to its home area or natal site to reproduce  
94 (Mayr, 1963; Greenwood, 1980), impacts the genetic structure of species, forming groups of  
95 individuals of similar matrilineage (Mourier & Planes, 2013; Stiebens et al., 2013).  
96 This strategy is common in the aquatic realm [e.g. salmonids (Dittman & Quinn, 1996),  
97 cetaceans (Engelhaupt et al., 2009), sharks (Hueter et al., 2005) and turtles (Bowen et al.,  
98 2005; Carreras et al., 2007; Lee, 2008)]. Particularly, sea turtles are capable of homing on a  
99 scale of a few kilometres (Lee et al., 2018). Upon hatching, neonate enter the ocean, find the  
100 major currents to actively escape predator-rich coastal waters (Scott et al., 2014; Putman &  
101 Mansfield, 2015; Putman et al., 2016), and disappear for a period known as the "lost years"  
102 (Carr, 1987). At sexual maturity, turtles return to their natal rookery likely using a combination  
103 of geomagnetic and olfactory cues (Brothers & Lohmann, 2015; Cameron et al., 2019).

104 Given this strong site fidelity, it is not surprising that some genomic regions demonstrate  
105 patterns of local adaptation (Stiebens et al., 2013).

106

107 Overall, despite philopatry, sea turtles have colonized various habitats over evolutionary  
108 timescales (Bowen & Karl, 2007). The loggerhead species (*Caretta caretta*) in particular is  
109 widely distributed in tropical and temperate regions, with nesting aggregations ranging from  
110 South Africa to Virginia (USA), including the world's largest rookeries located in Florida  
111 (USA, ~50,000 nests per year) and Masirah Island (Oman; ~30,000 nests/year, (Baldwin et  
112 al., 2003; Bolten & Witherington, 2004; Shamblin et al., 2014). The biogeography of Atlantic  
113 loggerheads was hypothetically shaped by geological and climatic events (Bowen & Karl,  
114 2007). The first of these events is the closure of the Isthmus of Panama that separated the  
115 Atlantic from the Pacific ~4.1 M years ago (Duchene et al., 2012; Shamblin et al., 2014).  
116 Since then, it has acted as a barrier for species that cannot tolerate freshwater conditions,  
117 preventing the movement between the Atlantic and the Pacific Oceans (Bowen et al., 1994;  
118 Bowen & Karl, 2007; Zanden et al., 2014). The second major biogeographic event refers to  
119 the warm water intrusions that have occurred during interglacial periods around the tip of  
120 South Africa, originating from the Agulhas Current (Turney & Jones, 2010). These inflows  
121 may have permitted the movement of loggerhead turtles from the Indian Ocean during  
122 interglacial periods. Reversely, when the cold Benguela current predominates in the region,  
123 low-temperature tolerance may prevent exchange between both ocean basins (Bowen &  
124 Karl, 2007).

125

126 There are currently two main hypotheses that explain the colonization history of loggerhead  
127 rookeries in the Atlantic. On the one hand, it has been proposed that the American rookery,  
128 ranging from southern Florida to Northern Carolina, is the oldest rookery in the Atlantic and  
129 among the firsts colonized - a conclusion drawn from the high haplotype and nucleotide  
130 diversity detected in this aggregation (Reis et al., 2010). On the other hand, Shamblin *et al.*  
131 (2014) suggested that the present Brazilian rookeries are the oldest in Atlantic, an hypothesis  
132 supported by the basal position of Brazilian mitochondrial DNA (mtDNA) haplotypes in a very  
133 large haplotype network (Shamblin et al., 2014). Either way, those events are reflected in the  
134 loggerheads' phylogeny and population structure, which is characterized by the existence of  
135 two divergent mtDNA haplogroups as well as genetic differentiation among rookeries within  
136 the ocean basin (Bowen et al., 1994; Bowen & Karl, 2007; Shamblin et al., 2014),.

137

138 Interestingly, the role of the Eastern Atlantic rookery in a colonization scenario remains to be  
139 completely understood (Shamblin et al., 2014). The Eastern Atlantic supports the third  
140 largest nesting aggregation of loggerhead turtles in the Archipelago of Cabo Verde (Marco et

141 al., 2012). The Cabo Verde archipelago is located approximately 500km off the Western  
142 coast of Africa. It consists of 10 volcanic islands with the oldest ~20My in the East (Maio) and  
143 the youngest aged of ~8My in the West (Pim et al., 2008). There, turtles lay ~15.000 nests  
144 per year (Marco et al., 2012). The majority of nesting events occurs on the island of Boavista,  
145 Maio, Sal and tends to reduce westwards. The existence of two very divergent lineages  
146 suggests that at least two independent colonization events occurred (Monzon-Arguello et al.,  
147 2010; Stiebens et al., 2013). Similarly, the asymmetric distribution of turtle density in the  
148 archipelago calls for the investigation of the directionality of gene flow to better understand  
149 the pattern of distribution of genetic diversity. Such knowledge will determine the source and  
150 sink nesting groups, facilitating management of this rookery. Nesting density on a smaller  
151 geographic scale is also heterogeneous: a beach of 15km length along the south eastern  
152 coast of Boavista island supports around >50% of all nesting activity in Cabo Verde (Marco  
153 et al., 2012).

154

155 In this study, we conducted population genetic analyses on loggerhead rookeries ranging  
156 from the large geographic scale of the Atlantic Ocean and Mediterranean Sea, to the regional  
157 scale of the Cabo Verde archipelago, and to the local scale of the Island of Boa Vista. We  
158 aimed to 1) revisit hypotheses of Atlantic colonization in order to clarify the role of Cabo  
159 Verde rookery in the process using hypothesis-driven population genetics modelling, 2) to  
160 determine the impact of philopatry on genetic diversity and demographic parameters at  
161 various geographical scales from the archipelago to an island level.

162

## 163 **Material and methods**

164

### 165 *Global screen for mitochondrial sequences*

166 Sequences of the mitochondrial control region were obtained both from previously published  
167 studies as well as by our own data collection for Cabo Verde. The objective was to obtain a  
168 robust representation of the rookeries of loggerhead turtles in the Atlantic and the  
169 Mediterranean Sea. We retrieved 521 sequences from rookeries in the Mediterranean Sea  
170 (Carreras et al., 2007; Clusa et al., 2013; Garofalo et al., 2013; Clusa et al., 2014), 2107 from  
171 the USA, which included the whole South Eastern Coast from South Florida to North  
172 Carolina (Shamblin et al., 2014) (Monzon-Arguello et al., 2010), 131 for the Brazilian rookery  
173 (Shamblin et al., 2014), 175 from Mexico (Shamblin et al., 2014) and 392 others from  
174 published studies in Cabo Verde (Monzon-Arguello et al., 2010; Stiebens et al., 2013;  
175 Shamblin et al., 2014). In total, 3326 sequences were obtained from published literature  
176 (supplementary file S1).

177

178 *Field sampling, DNA extraction and sequencing of mitochondrial control region from Cabo*  
179 *Verde*

180 To complement the dataset and improve the resolution at the regional level, field surveys  
181 took place in the Cabo Verde archipelago in 2011, 2012 and 2013 during the nesting  
182 seasons from June to October. Nine different islands were sampled: Boavista, Fogo, Maio,  
183 Sal, Santa Luzia, Santiago, Santo Antao, São Nicolau and São Vicente. On the island of  
184 Boavista, where the turtle density is the highest (Marco et al., 2012), we sampled on eight  
185 different beaches in order to investigate the genetic structure at a local scale. In total, we  
186 collected 881 samples from nesting loggerhead females. Samples consisted in removing  
187 3mm piece of non-keratinized tissue from the right front flipper using a single-use disposable  
188 scalpel. Samples were immediately stored in ethanol. Turtles were tagged with metal tags  
189 and/or pit tags directly after egg deposition to track nesting behaviour and to avoid multiple  
190 sampling (Stiebens et al., 2013). In the laboratory, each sample was washed in distilled  
191 water for about 20 seconds and cut into smaller pieces. DNA was extracted using the  
192 DNeasy® 96 Blood & Tissue Kit (QIAGEN, Hilden, Germany). Elution was conducted in twice  
193 75 µl of AE Buffer. All other steps followed the manufacturer's protocol.

194 The long fragment (~800bp) of control region of the mitochondrial DNA was amplified using  
195 the Primers LCM15382 (5'-GCTTAACCCTAAAGCATTGG-3') and H950 (5'-  
196 GTCTCGGATTTAGGGGTTTG-3') (Monzon-Arguello et al., 2010). A 10 µl PCR reaction  
197 consisted of 1µl 10x Buffer, 1 µl dNTP's (10 mM), 0.3 µl MgCl<sub>2</sub> (5nM), 3.6 µl HPLC water, 0.1  
198 µl Taq Polymerase (Invitex®), 1µl of each primer (5pmol/µl) and 1µl template DNA (~20µg).  
199 The reactions were carried out under the following thermo-cycling conditions: An initial  
200 denaturation step of 95°C for 2 minutes, followed by a second cycle that was repeated 40  
201 times with denaturation at 95°C for 30 seconds, annealing at 55°C for 30 seconds and  
202 elongation at 72°C for 1 minute. A final elongation step of 7 minutes at 72 °C was carried out.  
203 PCR products were cleaned with ExoSAP-IT® following the manufacturer's protocol. Cycle  
204 sequencing reactions were performed with Big Dye® Terminator v3.1 Cycle Sequencing Kit  
205 (Applied Biosystems, Darmstadt, Germany). Sequences were obtained from the forward  
206 direction (primer LCM15382). Where insufficient fragment lengths were retrieved, sequences  
207 from the reverse direction were also obtained and sequences were concatenated into  
208 contigs. Sequencing was performed with an ABI 3730 Genetic Analyzer (Applied  
209 Biosystems, Darmstadt, Germany). Sequences were assembled in Codon Code Aligner v5.0  
210 (CodonCode Corporation, Dedham, Massachusetts) and ambiguities were corrected by  
211 hand. All the amplified mitochondrial sequences were classified accordingly to the  
212 standardized nomenclature of the Archie Carr Centre for Sea Turtle Research  
213 (<http://accstr.ufl.edu>). The entire data set was aligned in Muscle v8.3.1 (Edgar, 2004). All  
214 unique sequences can be found in supplementary file S1.

215

## 216 ***On the large-scale rookeries of the Atlantic basin***

217

### 218 *Genetic diversity and population structure*

219 Haplotype (Hap) and nucleotide diversity ( $\pi$ ) indices were computed in Arlequin v3.5.1.3 for  
220 each of the major rookeries in the Atlantic and Mediterranean Sea (Excoffier et al., 2005).  
221 Relationship among haplotypes was investigated in a neighbour-joining network using  
222 Network v4.6.1.3 (<http://www.fluxus-engineering.com>), and visualized with PopArt  
223 (<http://popart.otago.ac.nz>). Population structure amongst those major rookeries was  
224 investigated using  $F_{ST}$  estimates in Arlequin v3.5.1.3 (10,000 permutations). Because the  
225 Cabo Verde rookery has still not been properly placed in the broader context of rookeries'  
226 structure, we performed a hierarchic Analysis of Molecular Variance (AMOVA) considering  
227 different grouping scenarios, i.e. grouping Cabo Verde with all rookeries separately. The  
228 considered rookeries were Brazil, Mediterranean Sea, Mexico and USA. Most likely grouping  
229 was identified based on the  $F_{CT}$ .

230

### 231 *Testing the ancestry of Atlantic and Mediterranean rookeries*

232 Rookeries' ancestry and colonization routes within the Atlantic basin and the Mediterranean  
233 Sea were explored by comparing the likelihood ratios of model-based inferences.  
234 Phylogenetic models were alternatively built with either the Mediterranean, Mexican, Cabo  
235 Verdean, USA and the Brazilian rookery as fixed at the root of the tree. The initial tree root  
236 height was set to initial split between the genus *Caretta* and the genus *Lepidochelys*, 4.09  
237 million years before present (Duchene et al., 2012). Monophyly was enforced in all rookeries  
238 in order to constrain tree topology during the course of MCMC sampling. These analyses  
239 were performed in BEAST v.1.8 (Drummond & Rambaut, 2007) and based on haplotype  
240 sequences without considering their frequencies. The substitution model was set to HKY as it  
241 was found to be the best-fit model of nucleotide substitution chosen through Akaike  
242 Information Criteria (AICc) in Mega v6.06 (Tamura et al., 2013) and the mutation rate was set  
243 to  $3.24 \times 10^{-3}$  substitutions/site/million year, as estimated for marine turtles (Duchene et al.,  
244 2012). The tree prior was set to coalescent and constant size. The MCMC chain length was  
245 set to  $10^8$  steps. Convergence was inspected in Tracer v1.6 (Rambaut et al., 2014), and  
246 models were compared by applying the AICM criteria (1000 bootstraps) (Baele et al., 2012).

247

### 248 *Testing colonization scenarios within the Atlantic Basin*

249 To complement the Bayesian phylogenies intended to infer the most likely ancestral rookery,  
250 we built possible colonization models in order to 1) strengthen phylogenetic conclusions and  
251 2) infer colonization routes within the Atlantic basin. Colonization hypotheses were tested

252 with models that weight the roles of migration, i.e. gene flow, and mutations as sources of  
253 genetic novelty within a population. Colonization models were built and compared in the  
254 software Migrate-n v.3.6 through Bayesian inference (Beerli & Felsenstein, 2001). Models  
255 consisted of different scenarios of rookeries serving as source of migrants, from which only  
256 emigration was allowed to occur. In total, we explored 12 possible colonization hypotheses  
257 (Fig. S1). Due to the extensive computation power required, we used only unique haplotype  
258 data in our preliminary screen. For these models, prior distribution for *gene flow* ( $M$ ) and  
259 *effective population size* ( $\theta$ ) were set as uniform with upper and lower boundaries explored  
260 by preliminary tests ( $\theta = 0 - 20$ ,  $M = 0 - 200$ ). Thermodynamic integration with 4 chains with  
261 different temperatures (1.0, 1.5, 3.0 and 1000000.0) was performed in order to improve the  
262 search for parameter space and allow comparisons of models with Bayes factor. A total of  
263  $5 \times 10^5$  steps were recorded in each chain after a burn-in of  $10^4$  states. Three independent  
264 replicates were performed for each scenario within each run, in order to ensure convergence.  
265 A total of  $1.5 \times 10^8$  parameters values were visited. Marginal likelihoods were used for model  
266 comparisons with Bayes Factor (Kass & Wasserman, 1995).

267 We further explored colonization hypothesis with approximate Bayesian computation  
268 implemented in the software DIYABC v2.1.0 (Cornuet et al., 2014). DIYABC allows the  
269 generation of simulated datasets and selection of those closest to the true dataset, and the  
270 estimate posterior distribution of specific statistics. The objective was to explore the  
271 possibility that the two major mtDNA haplogroups (CC1A and CC2A) may have distinct  
272 evolutionary and colonization histories after the split from a common ancestor. The genetic  
273 composition of contemporary Atlantic rookeries would therefore reflect several instances of  
274 secondary contact between proto-populations composed by individuals carrying haplotypes  
275 belonging to major haplogroup CC1 and CC2. DIYABC scenarios were built to test both  
276 migrate-n the 3 highest rank models and two others that could not be tested with migrate-n  
277 due to increased structure complexity.

278 In total, we constructed and compared 5 scenarios (Fig. 1). Reference tables were built with  
279 40.000.000 simulated datasets. Runs were optimized to search for the summary statistics  
280 with the least distance between simulated and observed dataset. Hence, we used all  $F_{ST}$   
281 pairwise comparisons between rookeries from the observed dataset to situate our data with  
282 the simulated parameter spaces of the 5 scenarios. Priors were defined as following: uniform  
283 population sizes min=100, max=500; uniform branching times (in generations) calibrated for  
284 the Last Glacial Maximum (LGM) at  $t_1$ , considering turtle generation time of 100 years and  
285 LGM taking place around 8000-12000ya. Thus,  $t_1$  min=80, max=100;  $t_2$  min=2000,  
286 max=3999;  $t_3$  min=4000, max=5999;  $t_4$  min=6000, max=8999 and  $t_5$  min=9000, max=10000.  
287 Mutation rate was also allowed to vary uniformly between  $10^{-3}$  and  $10^{-7}$ , with substitution  
288 model Kimura-2.



289

290

### 291 ***Regional level of the Cabo Verde archipelago***

292

#### 293 *Genetic diversity and structure within the Cabo Verde archipelago*

294 Arlequin v3.5.1.3 was used to calculate the nucleotide and haplotype diversity for each  
295 nesting group (i.e. each island), to compute Wright's fixation index ( $F_{ST}$ ) and perform exact  
296 tests for estimation of population differentiation (10.000 permutations). With the exception of  
297 calculating genetic indices, and to not influence direct comparisons due to exceptionally high  
298 sample size of Boavista, we randomly picked 100 sequences from Boavista and kept them  
299 for all downstream analyses. Results were corrected for multiple comparisons using the  
300 modified false discovery rate (FDR) method (Benjamini & Yekutieli, 2001), as suggested by  
301 Narum (Narum, 2006). Furthermore, we calculated the average  $F_{ST}$  for each nesting group in  
302 order to investigate whether a geographic pattern of population structure exists across the  
303 archipelago.

304

#### 305 *Demographic history and colonization scenarios within the Cabo Verde archipelago*

306 The demographic history of each nesting group was first investigated through moment  
307 estimates Tajima's D (computed with 1000 coalescent simulations), sum of squares deviation  
308 (SSD) and a measurement of goodness-of-fit, the raggedness index  $r$ . All these analyses  
309 were performed in Arlequin v3.5.1.3 and DNAsp v5.10(Librado & Rozas, 2009). Then,  
310 Bayesian skyline plots were constructed to infer fluctuations of effective population size  
311 throughout a temporal scale for each nesting group on each island. These were computed in  
312 BEAST v.1.8 (Drummond & Rambaut, 2007). The parameters substitution model and  
313 mutation rate were the same as the ones used in the phylogenetic scenarios. The initial tree  
314 root height and tree priors were also estimated in these analyses to have another  
315 perspective over colonization time for each island. Convergence was inspected in Tracer  
316 v1.6. Graphical display of the skylines was constructed in Tracer v1.6.

317 In order to further investigate the migration along the archipelago's West-East axis, we  
318 calculated the effective number of migrants (ENI) per generation across islands and related it  
319 to geographic distance and direction with a linear model (Stiebens et al., 2013). Migration  
320 estimates were obtained with migrate-n. For this model, prior distribution for *gene flow* (M)  
321 and *effective population size* ( $\theta$ ) were set as uniform with upper and lower boundaries of  $\theta =$   
322  $0 - 100$  and  $M = 0 - 1000$ . A total of  $10^6$  steps were recorded in each chain after a burn-in of  
323  $10^4$  states. Two independent replicates were performed for each scenario within each run. A  
324 total of  $2 \times 10^8$  parameters values were visited. We ran it three times, averaged  $\theta$  and M, and  
325 calculated effective migration rates (ENI) with the equation  $(\theta_{average} * M_{average})/2$ . Geographic

326 distances were calculated from the GPS coordinates of each island. Direction was inferred in  
327 relation to the longitudinal position of each island pair. ENIs and geographic distances were  
328 log transformed and incorporated in a linear model as response and explanatory variables,  
329 respectively, while direction (eastwards or westwards) of gene flow was incorporated as a  
330 factor. Statistical analyses were conducted in R v3.2.3 (Team, 2013).

### 331 ***Within beaches of Boavista***

#### 332 *Genetic diversity and structure within the island of Boavista*

333 Fine-scale variation in the distribution of genetic diversity was investigated for turtles nesting  
334 on the island of Boavista across 7 different beaches. Boavista is the eastern most island of  
335 the Archipelago and has an area of 631.1 km<sup>2</sup>. It is the Cabo Verdean Island where the  
336 majority of the nesting events takes place (Marco et al., 2012). Diversity indices (haplotype  
337 and nucleotide diversities), pairwise  $F_{ST}$  comparisons and exact tests of population  
338 differentiation amongst nesting beaches were computed in Arlequin v3.5.1.3. Bayesian  
339 skylines were performed as mentioned above. Test were corrected for multiple testing.

340

## 341 **Results**

342 Because some sequences retrieved from literature, as well as some obtained in this study,  
343 had different lengths, all sequences were trimmed to a consensus length of 674bp. This  
344 length does encompass the most polymorphic region of the control region (Monzon-Arguello  
345 et al., 2010). In total, we kept 521 sequences from the Mediterranean, 2107 from the USA,  
346 131 from Brazil, 175 from Mexico and 1273 from Cabo Verde. In total, this study includes  
347 4207 different sequences (Supplementary file S1).

### 348 ***On the large-scale rookeries of the Atlantic basin***

349

#### 350 *Diversity and population structure*

351 Indices of genetic diversity revealed that the Mexican loggerhead rookery exhibits the highest  
352 haplotype diversity ( $Hd_{\text{Mexico}} = 0.770$ ), while the USA rookery holds the highest value of  
353 nucleotide diversity ( $\pi_{\text{USA}} = 0.023$ ). The Mediterranean rookery showed the lowest values of  
354 haplotype ( $Hd_{\text{Mediterranean}} = 0.348$ ) and nucleotide diversity ( $\pi_{\text{Mediterranean}} = 0.001$ ), suggesting  
355 this rookery to be the most recently colonized or to be the result of fewer events of  
356 colonization. The Cabo Verdean rookery showed one of the highest indices of haplotype  
357 diversity ( $Hd_{\text{Cabo Verde}} = 0.572$ ) but one of the lowest of nucleotide diversity ( $\pi_{\text{Cabo Verde}} = 0.005$ )  
358 (Table 1). This contrasting reflects the important of placing the Cabo Verde Archipelago in  
359 the colonization history of the Atlantic Ocean by loggerhead turtles.

360 Not surprisingly given the philopatric nature of loggerhead turtles, pairwise  $F_{ST}$  comparisons  
361 among global rookeries revealed highly significant differentiation with  $F_{ST}$  values ranging from  
362 0.964 ( $p < 0.001$ ) between the rookeries of Brazil and the Mediterranean Sea to 0.303  
363 ( $p < 0.001$ ) between the rookeries of Cabo Verde and that of the USA (Fig. 2, Table S1). Exact  
364 tests of population differentiation showed similar results (Table 2). On average, the USA  
365 rookery showed the lowest, though highly significant, level of pairwise differentiation among  
366 all rookeries. None of the grouping scenarios tested with hierarchical AMOVA revealed  
367 significant  $F_{CT}$ , suggesting that this approach is not informative enough to infer the overall  
368 structure among rookeries.

### 369 *Ancestry and colonization routes of global rookeries*

370 To Infer ancestry and colonization routes across the Atlantic and into the Mediterranean Sea,  
371 we used phylogenetic models, where ancestry and monophyly were enforced sequentially for  
372 all rookeries. The comparison of marginal likelihoods of phylogenetic models with fixed  
373 ancestry suggested the USA rookery to be the oldest among all the ones analysed (Table  
374 S2). Noteworthy, all models showed very similar marginal likelihoods indicating weak  
375 statistical differences. Ranking AICM values across models strongly suggest the  
376 Mediterranean rookery to be youngest. Comparisons of migrate-n models based on Bayes  
377 factors revealed a model with an ancestral Mexico rookery from which turtles colonized all  
378 others, as well as a young Mediterranean rookery and a central Cabo Verde rookery acting  
379 as a stepping stone towards both sides of the Atlantic (best fit model M4, probability of 0.63,  
380 Fig S1, Table S3).

381 Approximate Bayesian computations revealed scenario S5 to be the most likely (Fig. S3).  
382 Scenario S5 suggests Brazil to be the most ancient rookery in the Atlantic, founded by an  
383 ancestral haplogroup I population that later colonized the Cabo Verdean rookery before a  
384 return towards the area of USA/Mexico. This S5 scenario further implies that the  
385 Mediterranean Sea was the last rookery to be founded but only by haplogroup II, whose  
386 individuals dispersed then to USA/Mexico and from there to Cabo Verde archipelago. Model  
387 inferences considering a lineage split prior to colonization and dispersal were never been  
388 attempted, and here we show that doing it allows the explore the likelihood of theorized  
389 colonization scenarios.

390

### 391 *Regional level of the Cabo Verde archipelago*

392

393 With Cabo Verde appearing as a central rookery acting as a stepping stone along the  
394 colonization of the Atlantic basin, we investigated the demographics, diversity and population

395 structure of this rookery. For the following analyses, we used 1273 mtDNA sequences of  
396 nesting female turtles. Twenty-two different haplotypes were detected, among them two  
397 haplotypes (UH5 and UH13, Supplementary File S1) that were found in previous study  
398 (Stiebens et al., 2013b) but not yet described in Genbank.

#### 399 *Demographic history of the archipelago*

400 Because demographic history may alter the understanding of the colonization patterns, we  
401 investigated the variation in various demographic indices for each nesting group (i.e. island)  
402 within the rookery. Results revealed two distinct patterns. The first one describes a possible  
403 population expansion in most of the northern set of islands of Sal, Santo Antao, Sao Nicolau,  
404 and Boavista. Together, with Fogo, all Tajima's were negative, non-significant SSD and  
405 raggedness indices (Table 3). However, only Sao Nicolau exhibited a significant Tajima's D.  
406 The other nesting groups rather experienced a constant population size or a decline as seen  
407 in Sao Vicente, Santiago, Santa Luzia and Maio islands (Table 3), and amongst those, only  
408 Sao Vicente showed a significant Tajima D.

409 Reconstructing the effective population size estimates from Bayesian skyline plots revealed  
410 that Sao Vicente, Boavista, Sao Nicolau and Sal showed a recent decline in effective  
411 population size followed by a possible recovery close to present time (Fig. 3). A possible  
412 demographic recovery is thus in line with negative Tajima D values. Nesting populations on  
413 the islands of Fogo, Maio, Santa Luzia, Santiago and Santo Antao instead show a relatively  
414 stable effective population size instead, where only in Maio and Santa Luzia did Tajima's D  
415 agreed with Bayesian skylines. Notably and despite all runs attained convergence, the  
416 observation that high probability density interval widens close to the present implies  
417 uncertainty regarding the current dynamics of each island's demography.

#### 418 *Diversity and structure of each island*

419 The most frequent haplotypes were CCA1.3 (n=766) and CCA17.1 (n=294) that belong to  
420 the oldest Haplotype I lineage. As expected, haplotype and nucleotide diversities show less  
421 variation at the regional level than at the global level, however they remain high and diverse  
422 (Table 3). Indices of genetic diversity split for nesting islands showed that turtles sampled in  
423 Sao Nicolau harbours the highest haplotype diversity ( $Hd_{SaoNicolau} = 0.681$ ) while those from  
424 Sao Vicente showed the highest nucleotide diversity ( $\pi_{SaoVicente} = 0.020$ ). Both islands belong  
425 to the northern area of the archipelago. The lowest values of haplotype diversity were  
426 observed in turtles from Santo Antao ( $Hd_{SantoAntao} = 0.438$ ) and the lowest nucleotide  
427 diversities were detected in turtles from four islands: Santo Antao, Santiago, Fogo and Maio  
428 ( $\pi = 0.001$ ) (Table 3). Noteworthy, the last three islands are adjacent in the South of the  
429 archipelago.

430 Pairwise  $F_{ST}$  comparisons among islands resulted in twelve statistically significant  
431 comparisons after correction for multiple comparisons (Fig. 2b). The genetic composition of  
432 Sao Vicente Island produced the highest  $F_{ST}$  values among island pairs, with statistically  
433 significant pairwise  $F_{ST}$  ranging from 0.174 with Fogo ( $p = 0.005$ ) to 0.294 with Maio ( $p <$   
434  $0.001$ ) (Table S4). Exact tests of population differentiation showed seventeen significant  
435 results, mostly consistent with pairwise  $F_{ST}$  particularly those involving the islands of Sao  
436 Vicente, Fogo and Sal (Table 4).  $F_{ST}$  did not correlate with geographic distance (Mantel test:  $r$   
437  $= -0.138$   $p=0.820$ ), suggesting an absence of isolation by distance.

438 Interestingly, the average pairwise  $F_{ST}$  was shown to significantly vary across islands  
439 (ANOVA:  $F = 4.367$ ,  $p < 0.001$ ), increasing in a linear fashion from East to West ( $R^2 = 0.275$ ,  
440  $p < 0.001$ , Fig. 4). To further describe the East-West pattern, we estimated the number of  
441 migrants amongst islands and the direction of gene flow. We found a significant interaction  
442 between the distance among islands and the direction of gene flow: the average number of  
443 migrants decreases eastwards ( $t_{\text{direction West}} = -1.281$ ,  $p = 0.047$ ) and increases westwards  
444 ( $t_{\text{direction West}} = 0.719$ ,  $p = 0.015$ ). This result demonstrates that the large nesting groups in the  
445 east mainly serve as source of migrants in the smaller nesting groups over evolutionary  
446 times (Fig. S3).

447

#### 448 ***Within beaches of Boavista***

449

450 The island of Boavista supports the largest nesting group in the Eastern Atlantic (Marco et  
451 al., 2012). We used the largest dataset collected from specific beaches in the island ( $N=626$ )  
452 to investigate the genetic diversity and population structure at the local scale (Table 1C). We  
453 found that the beach of *Agua Doce* showed the highest haplotype and nucleotide diversity  
454 ( $Hd_{\text{AguaDoce}} = 0.752$ ,  $\pi_{\text{AguaDoce}} = 0.009$ ), while Boa Esperança exhibited the lowest values in  
455 both indices ( $Hd_{\text{BoaEsperanca}} = 0.331$ ,  $\pi_{\text{BoaEsperanca}} = 0.001$ ). Interestingly, those beaches are  
456 adjacent to each other. Furthermore, haplotype diversity observed at the local scale was  
457 comparable to that of the regional level but reduced of about half for the nucleotide diversity  
458 (Table 5).

459 Surprisingly, pairwise comparisons were found significant at this local scale. All significant  
460 tests included the beach of Boa Esperança (Fig. 2c): Boa Esperança and Agua Doce ( $F_{ST} =$   
461  $0.220$ ,  $p = 0.00$ ), Boa Esperança and Curral Velho ( $F_{ST} = 0.062$ ,  $p = 0.00$ ), Boa Esperança  
462 and Lacacao ( $F_{ST} = 0.051$ ,  $p = 0.002$ ) and Boa Esperança and Norte ( $F_{ST} = 0.114$ ,  $p = 0.000$ )  
463 (Table S5). Given that we sampled 70 turtles from Boa Esperança, those significant results  
464 are unlikely to stem from small sample size.

465 All beaches of Boavista revealed a pattern of population expansion as suggested by negative  
466 Tajima's D and non-significant SSD and raggedness similar to the apparent scenario of  
467 population expansion detected in the above analyses for all the islands (Table 5). Bayesian  
468 skylines, however, revealed that Norte, Canto and Agua Doce might have experienced a  
469 short decline, while Boa Esperanca experienced a short expansion, when groups of turtles  
470 nesting on the other beaches showed no change in population size (Fig. S4).

## 471 **Discussion**

472 To effectively manage endangered species, it is crucial to understand the distribution of  
473 genetic diversity. In this study, we evaluated the genetic diversity of loggerhead sea turtle  
474 populations, known for their natal philopatric behaviours. Philopatry affects the distribution of  
475 genetic diversity since it reduces gene flow among populations. Nonetheless, the loggerhead  
476 turtle has colonized the entire Atlantic Ocean and the routes underlying this colonization are  
477 still elusive. Here, we show support for the Brazilian rookery to be the most ancient rookery  
478 in the Atlantic but support the idea that the colonization of the entire ocean basin occurred  
479 via two waves: one from the Pacific and other from the Indian. Each colonization event  
480 corresponds to that of a major haplotype group, both being now distributed across most of  
481 the Atlantic rookeries. Furthermore, we show that Cabo Verde rookery has played a key role  
482 in the colonization process, acting as a stepping stone facilitating the establishment of other  
483 rookeries on either side of the Atlantic. Focusing on Cabo Verde, we also show that the  
484 island supporting the largest nesting density is not necessarily that with the highest diversity  
485 indices. This is likely the result of an asymmetric functioning of the different nesting groups of  
486 the archipelago, with the Eastern islands acting as sources and the edge of the distribution  
487 mostly acting as sink. The eastern islands are those where turtle density is the highest and  
488 we find that because of strong philopatry, ~10kms accuracy, exchanges among islands are  
489 relatively rare.

### 490 *Revisiting the colonization of the Atlantic: a new perspective reconciles old hypothesis*

491 The existence of two highly divergent mitochondrial haplogroups that shape the  
492 phylogeographic patterns of the different ocean basins underlies the loggerhead's global  
493 biogeography (Bowen et al., 1994). The Atlantic being the youngest ocean basin, the  
494 unequal distribution of mtDNA haplogroups among rookeries suggests different colonization  
495 waves, as those lineages stem from the Indo-Pacific area (Shamblin et al., 2014). Therefore,  
496 to understand the colonization and posterior formation of the Atlantic rookeries, we  
497 considered those haplogroups as independent ancestral populations rather than forming one  
498 joint source of colonization. Modelling the temporal succession of haplogroup dispersal into  
499 and within the Atlantic with ABC reconciles current colonization hypotheses under a single  
500 scenario. More specifically, the most parsimonious succession of events suggest that the

501 Brazilian rookery was colonized first by individuals carrying haplotypes of major haplogroup I  
502 – probably a leakage from the Pacific into the Atlantic while the Central American Seaway  
503 was present. This was followed by the colonization of the Cabo Verdean archipelago and  
504 then the North and Central American rookeries of USA and Mexico. The first stage of Atlantic  
505 colonization is line with line with Shamblin et al (2014)'s hypothesis, as the Brazilian rookery  
506 is the oldest of the Atlantic and composed only by the turtles carrying haplotypes of group I.  
507 The colonization from Cabo Verde to northern Americas can be explained by the fact that  
508 warm saline waters were gradually introduced to northern latitudes as the Central American  
509 Seaway shallowed until total closure (Haug & Tiedemann, 1998). As loggerhead turtles  
510 require sand temperatures of at least 25° for successful incubation (Bowen & Karl, 2007),  
511 North American habitats might not have been suitable for nesting until after the closure of the  
512 isthmus of Panama.

513 On a more recent timescale, individuals carrying haplogroup II colonized the Mediterranean  
514 Sea. Likely after the last glaciations, migration occurred to Cabo Verde, where haplogroup II  
515 individuals established on already formed colonies, further proceeding to populate  
516 USA/Mexico. The pathway here presented thus supports Shamblin's et al (2014) hypothesis,  
517 specifically, the retention in the Indian ocean and subsequent entry via South Africa into the  
518 Atlantic (Shamblin et al., 2014). The major haplogroup II pathway favoured by the scenario  
519 modelling supports the nearly consensual hypothesis that Mediterranean Sea supports the  
520 youngest rookeries with access on the Atlantic Ocean (Clusa et al., 2014).

521 The biogeographic reconstruction of colonization pathways that assumes two distinct  
522 haplogroups as distinct ancestral populations clarifies key elements of the dispersal of  
523 loggerheads in the Atlantic. First, it rejects Central and North American rookeries as the  
524 oldest in the Atlantic. Notably, our summary statistics such as diversity indices and  $F_{ST}$ , as  
525 well as testing colonization hypothesis without segregating into haplogroups also suggested  
526 USA and/or Mexico as the oldest rookery. The apparent paradox can be explained by the  
527 physical convergence of the two divergent lineages in two waves of colonization in the area.  
528 The admixture of lineages from multiple genetic backgrounds is well known to increase  
529 diversity at sink populations (Roman & Darling, 2007). Thus, by being the last rookery to  
530 receive individuals carrying the highly diverse haplogroup I, USA/Mexico hold a signature  
531 that could be interpreted as that of an ancestral rookery, as observed by Reis et al (2010).  
532 Overall, the Atlantic can be understood as a secondary contact zone of major haplogroups  
533 that have accumulated divergence in allopatry. While we cannot exclude demographic  
534 effects that could have erased presence of genetic variants at local scale, one can  
535 parsimoniously assume that once admixed rookeries became established those would affect  
536 lineages equally.

537 *Colonization history, structure and demography of the Cabo Verdean rookery*

538 Regionally, the Cabo Verdean rookery shows both high haplotype and nucleotide diversities  
539 with the presence of both mtDNA lineages. Particularly, the island of Sao Vicente supports a  
540 nesting group with nucleotide diversity at least 3 times higher than that of other nesting  
541 groups of the archipelago. This is mainly linked to the presence of the most divergent lineage  
542 being frequent on this island. The presence of this haplotype can be traced mostly to one  
543 specific beach called Lazareto on the North-West of the island representing ~70% of the  
544 individuals. The presence of this Indo-Pacific haplotype, also present in the Mediterranean  
545 Sea- and interpreted as evidence for a second wave of colonization (Stiebens et al., 2013), is  
546 further reinforced by scenario simulations of the Atlantic colonization.

547 From a structure point of view, Cabo Verde was considered a single nesting population  
548 (Monzon-Arguello et al., 2010) and management unit (Wallace et al., 2011; Shamblin et al.,  
549 2014), while early signs of differentiations have been detected (Stiebens et al., 2013). The  
550 analyses of the more extensive dataset in this study confirms the highly significant genetic  
551 differentiation congruent with both  $F_{ST}$  and exact tests. This structure arises clearly from the  
552 island of Sao Vicente and the frequent divergent haplotype but not only. Indeed, a clear  
553 geographic pattern is visible where the islands from the western range of the archipelago  
554 show increased average differentiation compared to those of the eastern range. Noteworthy,  
555 signatures on mtDNA stem from female-mediated gene flow. Because bi-parentally inherited  
556 markers show an increase gene flow eastwards linked to opportunistic mating from Western  
557 males encountering more females on the east (Stiebens et al., 2013), our results suggest  
558 that the densely-populated easternmost islands of Sal, Boavista and Maio are extremely  
559 important in maintaining the functioning of the rookery, acting as evolutionary source  
560 populations. Here, we also reveal another geographic pattern, where gene flow of nesting  
561 females has propagated from the centre of the distribution to the edge. This pattern might be  
562 the ancient signature of colonization within the Archipelago: after the evolution of site fidelity  
563 to the firstly colonized islands, populations were established in all others through sporadic  
564 nesting events from the long-distance migrants, as it has recently been described to occur in  
565 Mediterranean rookeries (Carreras et al., 2018). Altogether, the observed genetic structure is  
566 the likely result of a strong female philopatric behavior as often observed in loggerhead  
567 turtles (FitzSimmons et al., 1997; Lee et al., 2007).

568 From a demographic perspective, estimates of effective population size suggest that after a  
569 small decline, the largest nesting groups are expanding. This is particularly the case for an  
570 East-West corridor entailing Boavista to Sao Vicente islands. While dating the decline is  
571 complex, the Cabo Verde rookery may hold the signature of intense poaching which has  
572 significantly impacted the census population size (Marco et al., 2008). This signature does



573 not necessarily represent the recent poaching peaks of the 1990s and 2000s. Instead, it may  
574 be the footprint of poaching activity, known since the human occupation of the archipelago in  
575 the 15<sup>th</sup> century (Loureiro & Torrão, 2008). However, demographic estimates should be  
576 interpreted with caution: the wide high probability density intervals observed for Bayesian  
577 skylines and non-significant Tajima D does not support conclusive evidence. Thus,  
578 conservation driven actions should be maintained in the Archipelago as well as monitoring of  
579 loggerheads census population sizes.

#### 580 *Philopatry at a fine geographic scale: structure and demography of the island of Boavista*

581 At the local scale, our results show that turtles nesting on one beach of the island of  
582 Boavista, Boa Esperança, harbour the lowest nucleotide diversity. This beach is situated  
583 about 12kms away from Ponta Ervatao & Ponta Cosme, the beaches with the highest  
584 nesting density in Cabo Verde and in the eastern Atlantic (>2500 nest per year, (Marco et al.,  
585 2012)). Reduced genetic diversity is likely the result of genetic isolation as demonstrated by  
586 the consistent significant differentiation of Boa Esperança with the surrounded beaches.  
587 Given that the sample size from this beach is ~70, this significant differentiation is unlikely to  
588 arise from random fluctuation linked to a small sample size. The parsimonious explanation is  
589 a high accuracy of philopatric behaviour on Boavista which can be detected away from the  
590 centre of the nesting activity, on the other side of the island, as the result of leakage of  
591 nesting behaviours.

#### 592 **Conclusion and future directions**

593 Our results offer a fresh perspective on the biogeography of the loggerhead sea turtle.  
594 Understanding the Atlantic as a secondary contact zone for two highly divergent lineages  
595 showed that ongoing hypothesis can be merged into a single colonization and dispersal  
596 scenario. The expansion pattern exposed allows to investigate major climatic and geological  
597 changes that shaped the pathways of colonization - such as the impact of the gradual  
598 closure of the isthmus of Panama in opening suitable nesting habitats at Northern latitudes.  
599 Our work also suggests that interpreting ancestry from genetic diversity estimates should be  
600 made with caution. As we have shown here, the presence of divergent lineages does not  
601 necessarily imply ancestry. Hypothesis testing with population genetic modelling may help to  
602 clarify conflicting views on the global biogeography.

603 Despite extensive migration, significant degrees of population differentiation spanned all the  
604 analysed geographic levels. Therefore, we have demonstrated that turtles are capable of  
605 extreme site fidelity and forming independent nesting groups at highly localized geographic  
606 scale. We identified two mechanisms. At the small scale, leakage away from the main  
607 nesting sites results in expansion. This mechanism yet relies on large population size, which

608 may be problematic for endangered species. The second mechanism of expansion relates to  
609 major climatic/geological events which requires the persistence of the species on a long  
610 evolutionary time.

611

612 **Acknowledgments.** The authors would like to thank the team members and volunteers of  
613 Biosferal, Caretta Caretta, Fondation Biodiversity Maio, National Institute for the  
614 Development of Fisheries (INDP), Projecto Vito Fogo, Projecto Vito Porto Novo, Project  
615 Biodiversity and Turtle Foundation who assisted with field work. The study was supported by  
616 a National Geographic grant (GEFNE69-13) and Queen Mary University Funds allocated to  
617 CE. MBS is currently supported by the FCT strategic project UID/MAR/04292/2013 granted  
618 to MARE. All applicable institutional and/or national guidelines for the care and use of animal  
619 were followed. The work was performed under DGA legislation of Cabo Verde  
620 (authorizations DGA 30/13, 040/GP/INDP/14).

#### 621 **Data accessibility statement**

622 All sequences obtained specifically for this study will be deposited in NCBI's nucleotide  
623 database.

624 **Author contributions.** CE, JDK and MBS designed the study. CSM, RT, TAA, MRS, DPL,  
625 DJ, PLJ, DH, CSJK, SVA and CE conducted field work in Cabo Verde. MBS and JDK  
626 performed the analysis with CE guidance. MBS drafted the manuscript with CE and JDK. All  
627 authors approved the final version of the manuscript.

628

629 **Tables**

630

631 **Table 1 – Diversity indices of major nesting aggregations of the Atlantic Ocean**, Abbreviations stand as  
 632 following: n=number of individual analysed, nHap=number of haplotypes, Hd=haplotype diversity,  
 633  $\pi$ =nucleotide diversity.

634

<i>Rookery</i>	<i>n</i>	<i>nHap</i>	<i>Hd</i>	$\pi$
Brazil	131	3	0.467	0.001
Cabo Verde	1273	20	0.572	0.005
Mediterranean	521	13	0.348	0.001
Mexico	175	14	0.770	0.015
USA	2107	23	0.555	0.023

635

636

637 **Table 2 – Exact population differentiation tests among rookeries.** In bold, significant values for  
 638  $p < 0.01$ .

	<i>Mexico</i>	<i>USA</i>	<i>MED</i>	<i>CV</i>
USA	<b>0.000</b>			
MED	<b>0.000</b>	<b>0.000</b>		
CV	<b>0.000</b>	<b>0.000</b>	<b>0.000</b>	
BRA	<b>0.000</b>	<b>0.000</b>	<b>0.000</b>	<b>0.000</b>

639

640 **Table 3 – Diversity indices for the islands of Cabo Verde.** Abbreviations stand as following:  
 641 n=number of individual analysed, nHap=number of haplotypes, Hd=haplotype diversity,  $\pi$ =nucleotide  
 642 diversity, SSD=sum of squared differences from mismatch distribution, r=ruggedness index. In  
 643 bold, significant values for  $p < 0.05$ .

<i>Island</i>	<i>n</i>	<i>nHap</i>	<i>Hd</i>	$\pi$	<i>Tajima's D</i>	<i>SSD</i>	<i>r</i>
Boavista (BV)	831	16	0.564	0.004	-1.486	0.067	0.269
Fogo (FG)	26	4	0.640	0.001	-0.390	0.004	0.089
Maió (MAI)	101	8	0.566	0.001	0.074	0.061	0.255
Sal (SI)	100	8	0.582	0.007	-0.964	0.027	0.118
Sao Nicolau (SN)	24	6	0.681	0.006	<b>-2.222</b>	0.009	0.041
Sao Vicente (SV)	65	10	0.662	0.020	<b>2.189</b>	0.112	0.171
Santa Luzia (SU)	55	3	0.560	0.002	0.879	0.039	0.147
Santiago (ST)	11	3	0.564	0.001	1.176	0.053	0.251
Santo Antao (SA)	60	5	0.438	0.001	-0.760	0.000	0.113

644

645 **Table 4 - Exact population differentiation tests among islands of the Cabo Verde Archipelago.** In

646 bold, significant values for  $p < 0.05$ .

647

	<i>Boavista</i>	<i>Sal</i>	<i>Sao Vicente</i>	<i>Sao Nicolau</i>	<i>Fogo</i>	<i>Maio</i>	<i>Santa Luzia</i>	<i>Santo Antao</i>
Sal	0.140							
Sao Vicente	0.000	<b>0.000</b>						
Sao Nicolau	0.039	0.195	0.076					
Fogo	<b>0.001</b>	<b>0.007</b>	<b>0.000</b>	0.098				
Maio	0.335	0.020	<b>0.000</b>	<b>0.006</b>	<b>0.003</b>			
Santa Luzia	0.151	0.029	<b>0.000</b>	<b>0.006</b>	<b>0.000</b>	0.100		
Santo Antao	<b>0.000</b>	<b>0.000</b>	<b>0.000</b>	<b>0.009</b>	<b>0.000</b>	<b>0.000</b>	<b>0.000</b>	
Santiago	0.933	0.764	0.237	0.623	0.326	0.777	0.747	0.015

648

649 **Table 5 - Diversity indices for beach in Boavista.** Abbreviations stand as following: n=number of

650 individual analysed, nHap=number of haplotypes, Hd=haplotype diversity,  $\pi$ =nucleotide diversity,

651 SSD=sum of squared differences from mismatch distribution, r=raggedness index. In bold,

652 significant values for  $p < 0.05$ .

653

<i>Beach</i>	<i>n</i>	<i>nHap</i>	<i>Hd</i>	$\pi$	<i>Tajima's D</i>	<i>SSD</i>	<i>r</i>
Agua Doce (AD)	15	5	0.752	0.009	<b>-2.005</b>	0.024	0.065
Boa Esperanca (BE)	70	6	0.331	0.001	-0.871	0.059	0.465
Canto (CA)	35	5	0.51	0.004	<b>-2.374</b>	0.118	0.474
Curral Velho (CuVe)	211	9	0.571	0.003	<b>-2.043</b>	0.088	0.333
Lacacao (La)	85	10	0.612	0.003	<b>-2.285</b>	0.030	0.121
Norte (No)	21	6	0.695	0.006	<b>-2.209</b>	0.043	0.145
Ponta Pesqueira (PP)	189	7	0.509	0.005	-1.179	0.090	0.384

654

655

656

657

658

659

660

661

662

663 **Table 6 - Exact population differentiation tests among the beaches in Boavista.** In bold, significant

664 values for  $p < 0.05$ .

	<i>Agua</i>		<i>Curral</i>			<i>Ponta</i>
	<i>Doce</i>	<i>Canto</i>	<i>Velho</i>	<i>Lacacao</i>	<i>Norte</i>	<i>pesqueira</i>
Canto	0.028					
Curral Velho	0.035	0.169				
Lacacao	0.283	0.350	0.286			
Norte	0.763	0.178	0.023	0.140		
Ponta						
pesqueira	<b>0.002</b>	0.085	0.023	<b>0.001</b>	0.011	
Boa Esperanca	<b>0.000</b>	0.117	<b>0.000</b>	<b>0.001</b>	<b>0.000</b>	<b>0.000</b>

665

666

667

668

669 **Figure legends**

670

671 **Figure 1 – Explored scenarios considering two colonization routes into the Atlantic**

672 The most complex scenarios drawn to test the hypothetical two waves of colonization  
673 stemming from two ancestral populations composed by the major haplogroup lineages are  
674 depicted. Time points ( $t_0$  to  $t_5$ ) of each split are the same across scenarios and are all  
675 relative to the initial split that occurred at  $t=5$ . Proto populations refer to ancestral populations  
676 prior to lineage admixture;  $ra$  and  $1-ra$  refer to the ratio of individuals from each ancestral  
677 population used to originate the new populations. The pairwise  $F_{ST}$  between rookeries  
678 estimated from each scenario were then compared to the observed pairwise  $F_{ST}$ . The  
679 scenario best explaining  $F_{ST}$  distribution is depicted with a star.

680 **Figure 2 – Pairwise  $F_{ST}$  distribution across the three geographic scales**

681 Heatmap of the pairwise  $F_{ST}$  among (a) major rookeries in the Atlantic basin, (b) islands of  
682 the Cabo Verde archipelago, and (c) beaches of Boavista (c). Statistically significant pairwise  
683 comparisons are represented with \*\*\* for  $p<0.001$  and with \*\* for  $0.001<p<0.01$ .

684 **Figure 3 – Bayesian Skyline Plots (BSPs) for the nine islands of Cabo Verde**

685 Effective population size across evolutionary timescales for each island. Y-axis is an  
686 estimate of the product of  $N_e$  \* mutation rate ( $\mu$ ) per generation, while the x-axis represents a  
687 relative temporal scale. Note that the differences in x-axis scale across graphs reflect the  
688 putative age of the genealogy. The black line represents the mean  $N_e$  and the blue shading  
689 the 95% high probability density interval. There is an inflection points for Boavista and Sao  
690 Vicente populations, suggestive of an increase after a population decline. The islands of Sal  
691 and Sao Nicolau present a declining trend and the aggregations on the remaining islands  
692 suggest stability of effective population sizes in the respective time frames.

693 **Figure 4 – Distribution of average pairwise  $F_{ST}$  among the islands of the archipelago**

694 Linear regression of average pairwise  $F_{ST}$  per island along the East to West axis of the  
695 archipelago following the equation  $F_{ST} \sim Island$ . A significant increase in average pairwise  $F_{ST}$   
696 can be observed from East to West ( $R^2=0.275$ ,  $p<0.001$ ).

697

698

699

## 700 **Supplementary figure legends**

701

### 702 **Figure S1 – Global colonization models**

703 Hypothesized models of Atlantic colonization tested with migrate-n. **BRA**: Brazilian rookeries,  
704 **CV**: Cabo Verdean rookeries, **MEX**: Mexican rookeries, **USA**: North American rookeries;  
705 **MED**: Mediterranean rookeries. All biologically plausible combinations of unidirectional  
706 migration were tested.

### 707 **Figure S2 – Logistic regression comparison of scenarios modelled in diyABC**

708 Scenario comparison results of hypothesized two colonization routes into the Atlantic. In the  
709 x-axis is shown the number of simulated scenarios (in batches of 1000) whose mean  
710 pairwise  $F_{ST}$  is more approximate to that obtained with the observed dataset. The y-axis is  
711 the corresponded regression coefficient for sequential batches of 1000 points.

### 712 **Figure S3 – Relationship between migration estimates and geographic distance for 713 each direction**

714 X-axis shows the log-scaled geographic distance and the y-axis shows the effective  
715 migration rate for eastward (E) and westward (W) migration.

### 716 **Figure S4 – Bayesian Skyline Plots of Bovista's beaches**

717 Effective population size across evolutionary timescales for each island. Y-axis is an  
718 estimate of the product of  $N_e$  \* mutation rate ( $\mu$ ) per generation, while the x-axis represents a  
719 relative temporal scale. Note that the differences in x-axis scale across graphs reflect the  
720 putative age of the genealogy. The black line represents the mean  $N_e$  and the blue shading  
721 the 95% high probability density interval.

722

723



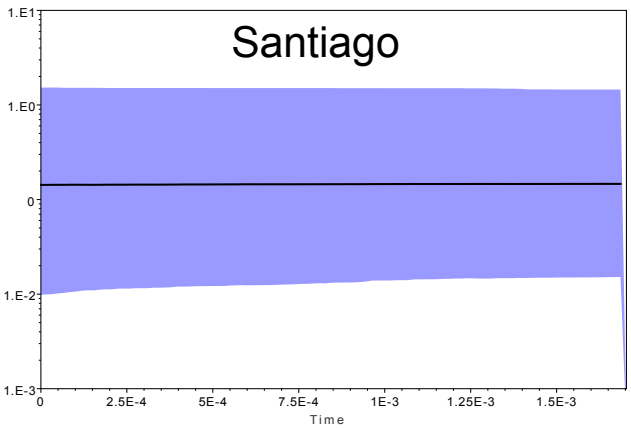
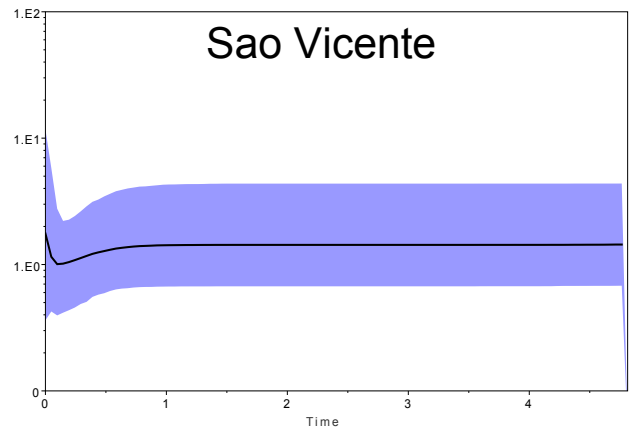
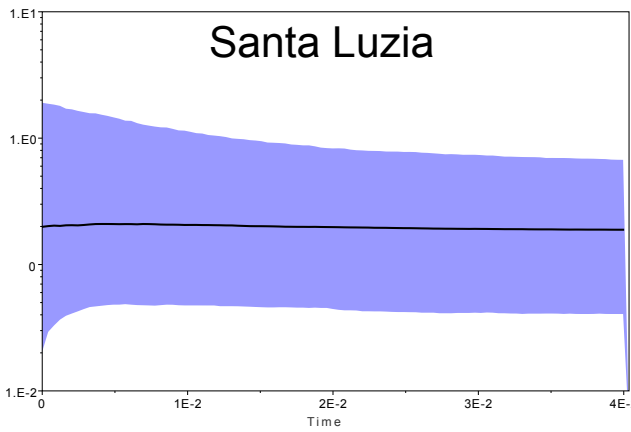
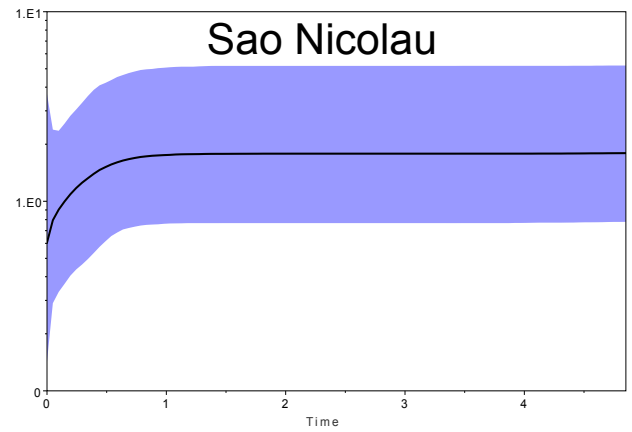
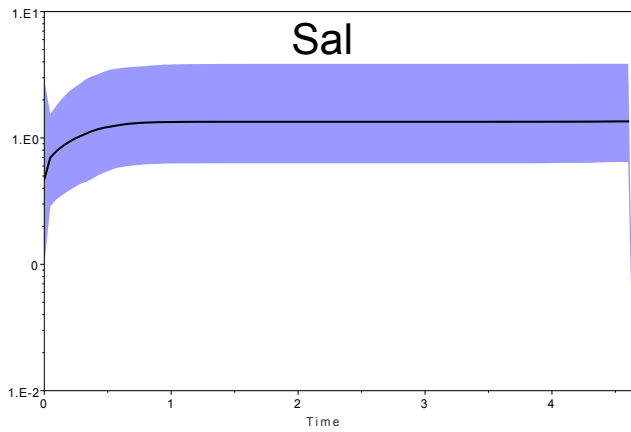
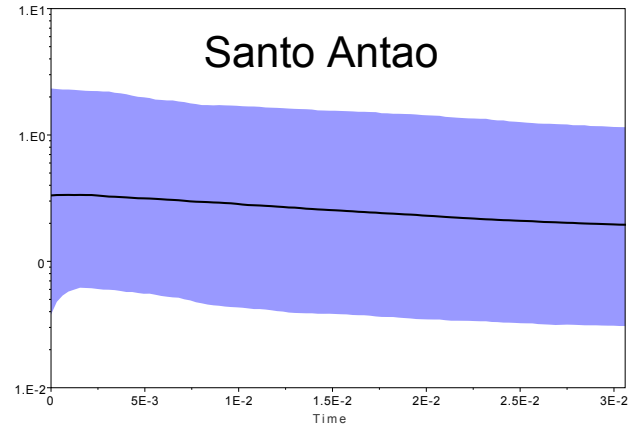
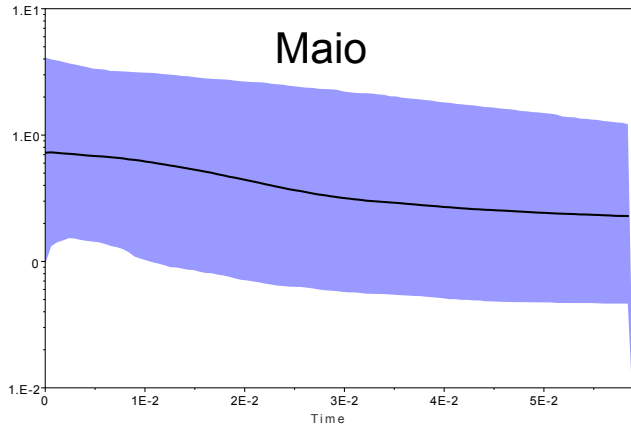
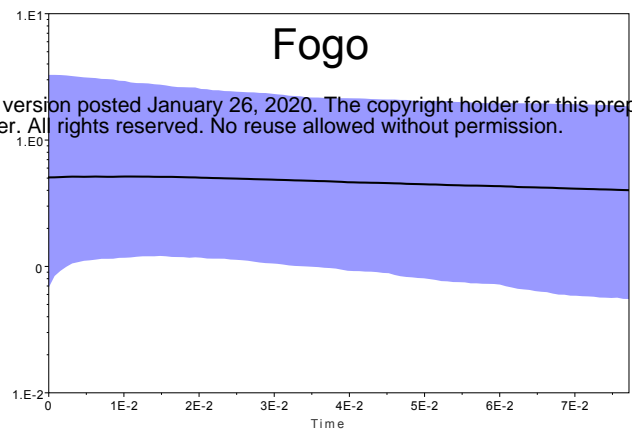
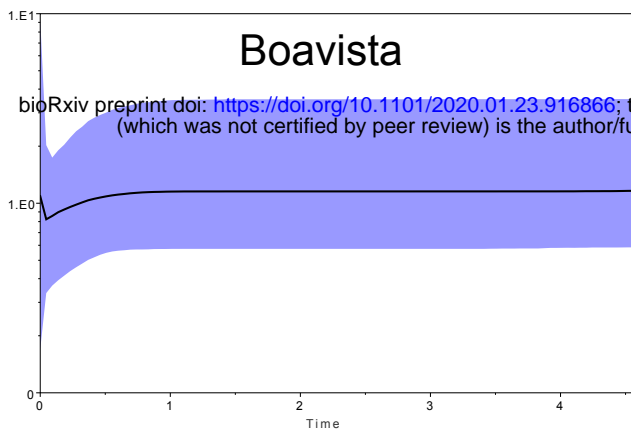
724 **References**

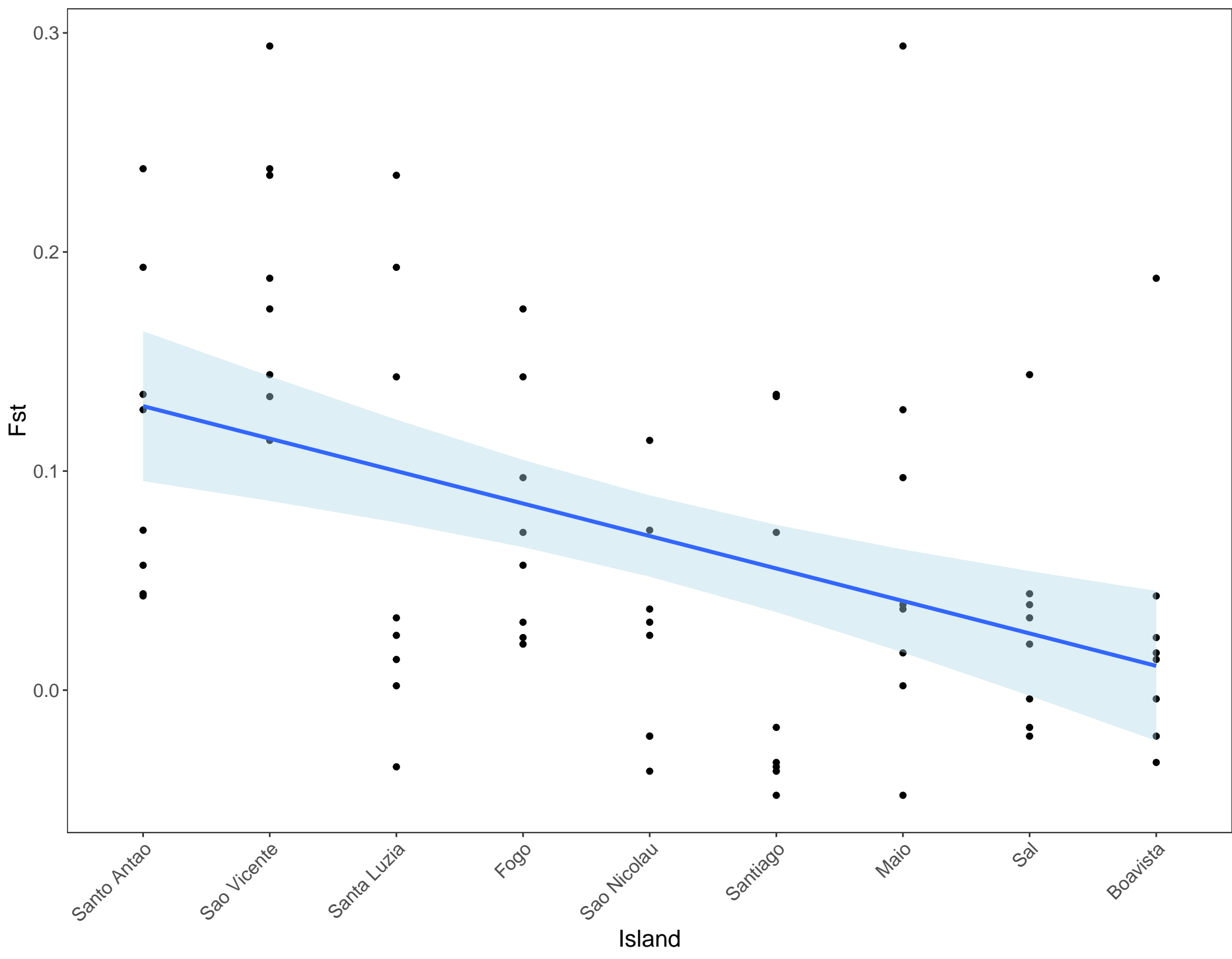
- 725 Baele, G., Lemey, P., Bedford, T., Rambaut, A., Suchard, M.A. & Alekseyenko, A.V. (2012)  
726 Improving the accuracy of demographic and molecular clock model comparison while  
727 accommodating phylogenetic uncertainty. *Molecular Biology and Evolution*, **29**, 2157-  
728 2167.
- 729 Baldwin, R., Hughes, G. & Prince, R. (2003) Loggerhead turtles in the indian ocean.  
730 *Loggerhead Sea Turtles. Smithsonian Institution Press, Washington, DC*, 218-232.
- 731 Beaumont, M.A., Nielsen, R., Robert, C., Hey, J., Gaggiotti, O., Knowles, L., Estoup, A.,  
732 Panchal, M., Corander, J. & Hickerson, M. (2010) In defence of model-based  
733 inference in phylogeography. *Molecular ecology*, **19**, 436-446.
- 734 Beerli, P. & Felsenstein, J. (2001) Maximum likelihood estimation of a migration matrix and  
735 effective population sizes in n subpopulations by using a coalescent approach.  
736 *Proceedings of the National Academy of Sciences of the United States of America*,  
737 **98**, 4563-4568.
- 738 Benjamini, Y. & Yekutieli, D. (2001) The control of the false discovery rate in multiple testing  
739 under dependency. *The Annals of Statistics*, **29**, 1165-1188.
- 740 Bolten, A.B. & Witherington, B.E. (2004) Loggerhead sea turtles. *Marine Turtle Newsletter*,  
741 **104**, 319pp.
- 742 Bowen, B.W. & Karl, S.A. (2007) Population genetics and phylogeography of sea turtles.  
743 *Molecular Ecology*, **16**, 4886-4907.
- 744 Bowen, B.W., Bass, A.L., Soares, L. & Toonen, R.J. (2005) Conservation implications of  
745 complex population structure: Lessons from the loggerhead turtle (*Caretta caretta*).  
746 *Molecular Ecology*, **14**, 2389-2402.
- 747 Bowen, B.W., Kamezaki, N., Limpus, C.J., Hughes, G.R., Meylan, A.B. & Avise, J.C. (1994)  
748 Global phylogeography of the loggerhead turtle (*Caretta caretta*) as indicated by  
749 mitochondrial-DNA haplotypes. *Evolution*, **48**, 1820-1828.
- 750 Brothers, J.R. & Lohmann, Kenneth J. (2015) Evidence for geomagnetic imprinting and  
751 magnetic navigation in the natal homing of sea turtles. *Current Biology*, **25**, 392-396.
- 752 Brunner, F.S., Deere, J.A., Egas, M., Eizaguirre, C. & Raeymaekers, J.A. (2019) The  
753 diversity of eco-evolutionary dynamics: Comparing the feedbacks between ecology  
754 and evolution across scales. *Functional ecology*, **33**, 7-12.
- 755 Cameron, S.J., Baltazar-Soares, M. & Eizaguirre, C. (2019) Region-specific magnetic fields  
756 structure sea turtle populations. *bioRxiv*, 630152.
- 757 Carotenuto, F., Di Febraro, M., Melchionna, M., Castiglione, S., Saggese, F., Serio, C.,  
758 Mondanaro, A., Passaro, F., Loy, A. & Raia, P. (2016) The influence of climate on  
759 species distribution over time and space during the late quaternary. *Quaternary  
760 Science Reviews*, **149**, 188-199.
- 761 Carr, A. (1987) New perspectives on the pelagic stage of sea turtle development.  
762 *Conservation Biology*, **1**, 103-121.
- 763 Carreras, C., Pascual, M., Tomás, J., Marco, A., Hochscheid, S., Castillo, J.J., Gozalbes, P.,  
764 Parga, M., Piovano, S. & Cardona, L. (2018) Sporadic nesting reveals long distance  
765 colonisation in the philopatric loggerhead sea turtle (*Caretta caretta*). *Scientific  
766 reports*, **8**, 1435.
- 767 Carreras, C., Pascual, M., Cardona, L., Aguilar, A., Margaritoulis, D., Rees, A., Turkozan, O.,  
768 Levy, Y., Gasith, A., Aureggi, M. & Khalil, M. (2007) The genetic structure of the  
769 loggerhead sea turtle (*Caretta caretta*) in the mediterranean as revealed by nuclear  
770 and mitochondrial DNA and its conservation implications. *Conservation Genetics*, **8**,  
771 761-775.
- 772 Clusa, M., Carreras, C., Pascual, M., Demetropoulos, A., Margaritoulis, D., Rees, A.F.,  
773 Hamza, A.A., Khalil, M., Aureggi, M., Levy, Y., Türkozan, O., Marco, A., Aguilar, A. &  
774 Cardona, L. (2013) Mitochondrial DNA reveals pleistocenic colonisation of the  
775 mediterranean by loggerhead turtles (*Caretta caretta*). *Journal of Experimental Marine  
776 Biology and Ecology*, **439**, 15-24.
- 777 Clusa, M., Carreras, C., Pascual, M., Gaughran, S.J., Piovano, S., Giacoma, C., Fernandez,  
778 G., Levy, Y., Tomas, J., Raga, J.A., Maffucci, F., Hochscheid, S., Aguilar, A. &

- 779 Cardona, L. (2014) Fine-scale distribution of juvenile atlantic and mediterranean  
780 loggerhead turtles (*Caretta caretta*) in the mediterranean sea. *Marine Biology*, **161**,  
781 509-519.
- 782 Cornuet, J.-M., Pudlo, P., Veyssier, J., Dehne-Garcia, A., Gautier, M., Leblois, R., Marin, J.-  
783 M. & Estoup, A. (2014) Diyabc v2. 0: A software to make approximate bayesian  
784 computation inferences about population history using single nucleotide  
785 polymorphism, DNA sequence and microsatellite data. *Bioinformatics*, **30**, 1187-1189.
- 786 Csillery, K., Blum, M.G.B., Gaggiotti, O.E. & Francois, O. (2010) Approximate bayesian  
787 computation (abc) in practice. *Trends in Ecology & Evolution*, **25**, 410-418.
- 788 Dittman, A. & Quinn, T. (1996) Homing in pacific salmon: Mechanisms and ecological basis.  
789 *The Journal of Experimental Biology*, **199**, 83-91.
- 790 Drummond, A.J. & Rambaut, A. (2007) Beast: Bayesian evolutionary analysis by sampling  
791 trees. *BMC Evolutionary Biology*, **7**, 214-214.
- 792 Drummond, A.J., Rambaut, A., Shapiro, B. & Pybus, O.G. (2005) Bayesian coalescent  
793 inference of past population dynamics from molecular sequences. *Molecular Biology  
794 and Evolution*, **22**, 1185-1192.
- 795 Duchene, S., Frey, A., Alfaro-Núñez, A., Dutton, P.H., Thomas P. Gilbert, M. & Morin, P.A.  
796 (2012) Marine turtle mitogenome phylogenetics and evolution. *Molecular  
797 Phylogenetics And Evolution*, **65**, 241-250.
- 798 Edgar, R.C. (2004) Muscle: A multiple sequence alignment method with reduced time and  
799 space complexity. *BMC Bioinformatics*, **5**, 113.
- 800 Eizaguirre, C. & Baltazar-Soares, M. (2014) Evolutionary conservation—evaluating the  
801 adaptive potential of species. *Evolutionary Applications*, **7**, 963-967.
- 802 Ellegren, H. & Galtier, N. (2016) Determinants of genetic diversity. *Nature Reviews Genetics*,  
803 **17**, 422.
- 804 Engelhaupt, D., Rus Hoelzel, A., Nicholson, C., Frantzis, A., Mesnick, S., Gero, S.,  
805 Whitehead, H.A.L., Rendell, L., Miller, P., De Stefanis, R., Cañadas, A.N.A., Airoldi,  
806 S. & Mignucci-Giannoni, A.A. (2009) Female philopatry in coastal basins and male  
807 dispersion across the north atlantic in a highly mobile marine species, the sperm  
808 whale (*Physeter macrocephalus*). *Molecular Ecology*, **18**, 4193-4205.
- 809 Excoffier, L., Laval, G. & Schneider, S. (2005) Arlequin (version 3.0): An integrated software  
810 package for population genetics data analysis. *Evolutionary Bioinformatics Online*, **1**,  
811 47-50.
- 812 Ezard, T.H., Aze, T., Pearson, P.N. & Purvis, A. (2011) Interplay between changing climate  
813 and species' ecology drives macroevolutionary dynamics. *Science*, **332**, 349-351.
- 814 FitzSimmons, N.N., Limpus, C.J., Norman, J.A., Goldizen, A.R., Miller, J.D. & Moritz, C.  
815 (1997) Philopatry of male marine turtles inferred from mitochondrial DNA markers.  
816 *Proceedings of the National Academy of Sciences of the United States of America*,  
817 **94**, 8912-8917.
- 818 Frankham, R., Briscoe, D.A. & Ballou, J.D. (2002) *Introduction to conservation genetics*.  
819 Cambridge university press.
- 820 Garofalo, L., Mastrogiacomo, A., Casale, P., Carlini, R., Eleni, C., Freggi, D., Gelli, D.,  
821 Knittweis, L., Mifsud, C., Mingozzi, T., Novarini, N., Scaravelli, D., Scillitani, G.,  
822 Oliverio, M. & Novelletto, A. (2013) Genetic characterization of central mediterranean  
823 stocks of the loggerhead turtle (*Caretta caretta*) using mitochondrial and nuclear  
824 markers, and conservation implications. *Aquatic Conservation: Marine and  
825 Freshwater Ecosystems*, **23**, 868-884.
- 826 Greenwood, P.J. (1980) Mating systems, philopatry and dispersal in birds and mammals.  
827 *Animal Behaviour*, **28**, 1140-1162.
- 828 Haug, G.H. & Tiedemann, R. (1998) Effect of the formation of the isthmus of panama on  
829 atlantic ocean thermohaline circulation. *Nature*, **393**, 673-676.
- 830 Hueter, R.E., Heupel, M.R., Heist, E.J. & Keeney, D.B. (2005) Evidence of philopatry in  
831 sharks and implications for the management of shark fisheries. *Journal of Northwest  
832 Atlantic Fishery Science*, **35**, 239-247.
- 833 Jackson, J.A., Steel, D.J., Beerli, P., Congdon, B.C., Olavarría, C., Leslie, M.S., Pomilla, C.,  
834 Rosenbaum, H. & Baker, C.S. (2014) Global diversity and oceanic divergence of

- 835 humpback whales (megaptera novaeangliae). *Proceedings of the Royal Society B:*  
836 *Biological Sciences*, **281**, 20133222.
- 837 Kass, R.E. & Wasserman, L. (1995) A reference bayesian test for nested hypotheses and its  
838 relationship to the schwarz criterion. *Journal of the american statistical association*,  
839 **90**, 928-934.
- 840 Lee, P.L., Luschi, P. & Hays, G.C. (2007) Detecting female precise natal philopatry in green  
841 turtles using assignment methods. *Molecular ecology*, **16**, 61-74.
- 842 Lee, P.L., Schofield, G., Haughey, R.I., Mazaris, A.D. & Hays, G.C. (2018) A review of  
843 patterns of multiple paternity across sea turtle rookeries. *Advances in marine biology*,  
844 pp. 1-31. Elsevier.
- 845 Lee, P.L.M. (2008) Molecular ecology of marine turtles: New approaches and future  
846 directions. *Journal of Experimental Marine Biology and Ecology*, **356**, 25-42.
- 847 Librado, P. & Rozas, J. (2009) Dnasp v5: A software for comprehensive analysis of DNA  
848 polymorphism data. *Bioinformatics*, **25**, 1451-1452.
- 849 Loureiro, N. & Torrão, M. (2008) Homens e tartarugas marinhas: Seis séculos de história e  
850 histórias nas ilhas de cabo verde. *Anais Hist. Além-Mar*, 37-78.
- 851 Loveless, M.D. & Hamrick, J.L. (1984) Ecological determinants of genetic-structure in plant  
852 populations. *Annual Review of Ecology and Systematics*, **15**, 65-95.
- 853 Marco, A., Carreras, C. & Castillo, J.J. (2008) A step towards the conservation of the  
854 loggerhead turtle of the atlantic. *Quercus*, **266**, 37-40.
- 855 Marco, A., Abella, E., Liria-Loza, A., Martins, S., Lopez, O., Jimenez-Bordon, S., Medina, M.,  
856 Oujo, C., Gaona, P., Godley, B.J. & Lopez-Jurado, L.F. (2012) Abundance and  
857 exploitation of loggerhead turtles nesting in boa vista island, cape verde: The only  
858 substantial rookery in the eastern atlantic. *Animal Conservation*, **15**, 351-360.
- 859 Mayr, E. (1963) *Animal species and evolution*. Harvard University Press, Cambridge.
- 860 Monzon-Arguello, C., Rico, C., Naro-Maciel, E., Varo-Cruz, N., Lopez, P., Marco, A. &  
861 Lopez-Jurado, L.F. (2010) Population structure and conservation implications for the  
862 loggerhead sea turtle of the cape verde islands. *Conservation Genetics*, **11**, 1871-  
863 1884.
- 864 Mourier, J. & Planes, S. (2013) Direct genetic evidence for reproductive philopatry and  
865 associated fine-scale migrations in female blacktip reef sharks (*carcharhinus*  
866 *melanopterus*) in french polynesia. *Molecular Ecology*, **22**, 201-214.
- 867 Narum, S.R. (2006) Beyond bonferroni: Less conservative analyses for conservation  
868 genetics. *Conservation Genetics*, **7**, 783-787.
- 869 Perry, A.L., Low, P.J., Ellis, J.R. & Reynolds, J.D. (2005) Climate change and distribution  
870 shifts in marine fishes. *Science*, **308**, 1912-1915.
- 871 Pim, J., Peirce, C., Watts, A.B., Grevemeyer, I. & Krabbenhoft, A. (2008) Crustal structure  
872 and origin of the cape verde rise. *Earth and Planetary Science Letters*, **272**, 422-428.
- 873 Portnoy, D., Hollenbeck, C., Belcher, C., Driggers III, W., Frazier, B., Gelsleichter, J., Grubbs,  
874 R. & Gold, J. (2014) Contemporary population structure and post-glacial genetic  
875 demography in a migratory marine species, the blacknose shark, *carcharhinus*  
876 *acronotus*. *Molecular ecology*, **23**, 5480-5495.
- 877 Putman, Nathan F. & Mansfield, Katherine L. (2015) Direct evidence of swimming  
878 demonstrates active dispersal in the sea turtle "lost years". *Current Biology*, **25**, 1221-  
879 1227.
- 880 Putman, N.F., Lumpkin, R., Sacco, A.E. & Mansfield, K.L. (2016) Passive drift or active  
881 swimming in marine organisms? *Proceedings of the Royal Society B: Biological*  
882 *Sciences*, **283**
- 883 Rambaut, A., Suchard, M.A., Xie, D. & Drummond, A.J. (2014) Tracer v1.6.. Available from  
884 <http://beast.bio.ed.ac.uk/Tracer>,
- 885 Reis, E., Soares, L., Vargas, S., Santos, F., Young, R., Bjorndal, K., Bolten, A. & Lôbo-  
886 Hajdu, G. (2010) Genetic composition, population structure and phylogeography of  
887 the loggerhead sea turtle: Colonization hypothesis for the brazilian rookeries.  
888 *Conservation Genetics*, **11**, 1467-1477.
- 889 Roman, J. & Darling, J.A. (2007) Paradox lost: Genetic diversity and the success of aquatic  
890 invasions. *Trends in ecology & evolution*, **22**, 454-464.

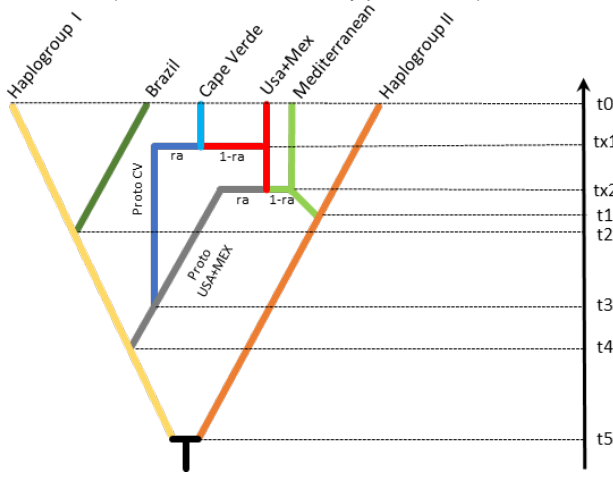
- 891 Scott, R., Marsh, R. & Hays, G.C. (2014) Ontogeny of long distance migration. *Ecology and*  
892 *Evolution, In Press*
- 893 Shamblin, B.M., Bolten, A.B., Abreu-Grobois, F.A., Bjorndal, K.A., Cardona, L., Carreras, C.,  
894 Clusa, M., Monzón-Argüello, C., Nairn, C.J. & Nielsen, J.T. (2014) Geographic  
895 patterns of genetic variation in a broadly distributed marine vertebrate: New insights  
896 into loggerhead turtle stock structure from expanded mitochondrial DNA sequences.  
897 *PLoS One*, **9**, e85956.
- 898 Stiebens, V.A., Merino, S.E., Roder, C., Chain, F.J.J., Lee, P.L.M. & Eizaguirre, C. (2013)  
899 Living on the edge: How philopatry maintains adaptive potential. *Proceedings of the*  
900 *Royal Society B: Biological Sciences*, **280**
- 901 Tamura, K., Stecher, G., Peterson, D., FilipSKI, A. & Kumar, S. (2013) Mega6: Molecular  
902 evolutionary genetics analysis version 6.0. *Molecular Biology and Evolution*,
- 903 Team, R.C. (2013) R: A language and environment for statistical computing.
- 904 Turney, C.S.M. & Jones, R.T. (2010) Does the agulhas current amplify global temperatures  
905 during super-interglacials? *Journal of Quaternary Science*, **25**, 839-843.
- 906 Wallace, B.P., DiMatteo, A.D., Hurley, B.J., Finkbeiner, E.M., Bolten, A.B., Chaloupka, M.Y.,  
907 Hutchinson, B.J., Abreu-Grobois, F.A., Amorocho, D., Bjorndal, K.A., Bourjea, J.,  
908 Bowen, B.W., Duenas, R.B., Casale, P., Choudhury, B.C., Costa, A., Dutton, P.H.,  
909 Fallabrino, A., Girard, A., Girondot, M., Godfrey, M.H., Hamann, M., Lopez-  
910 Mendilaharsu, M., Marcovaldi, M.A., Mortimer, J.A., Musick, J.A., Nel, R., Pilcher,  
911 N.J., Seminoff, J.A., Troeng, S., Witherington, B. & Mast, R.B. (2011) Regional  
912 management units for marine turtles: A novel framework for prioritizing conservation  
913 and research across multiple scales. *PLoS ONE*, **5**
- 914 Zanden, H.B.V., Pfaller, J., Reich, K., Pajuelo, M., Bolten, A., Williams, K., Frick, M.,  
915 Shamblin, B., Nairn, C. & Bjorndal, K. (2014) Foraging areas differentially affect  
916 reproductive output and interpretation of trends in abundance of loggerhead turtles.  
917 *Marine Biology*, **161**, 585-598.



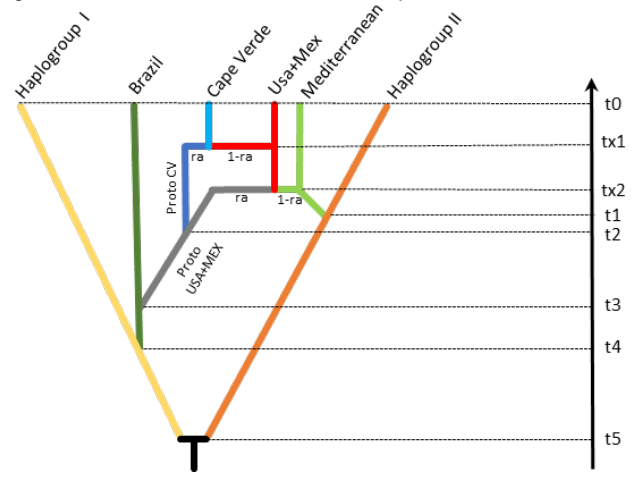


# Scenario I

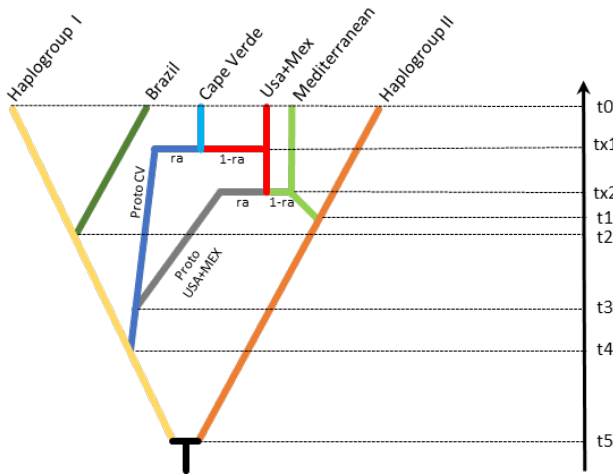
bioRxiv preprint doi: <https://doi.org/10.1101/2020.01.23.916866>; this version posted January 26, 2020. The copyright holder for this preprint (which was not certified by peer review) is the author/funder. All rights reserved. No reuse allowed without permission.



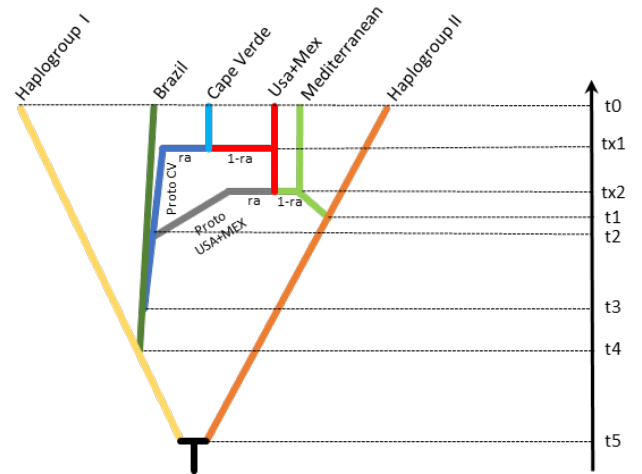
# Scenario II



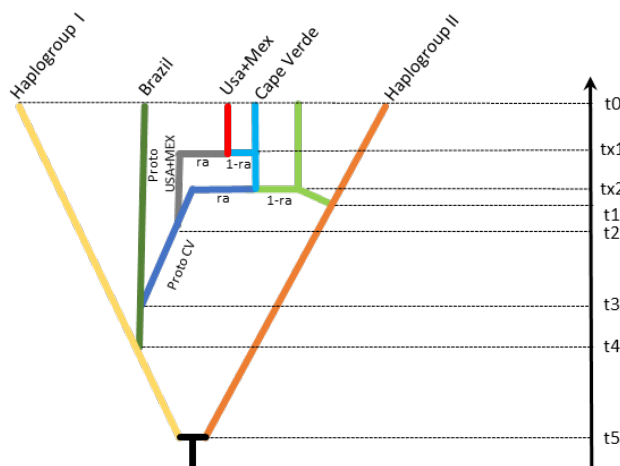
# Scenario III



# Scenario IV

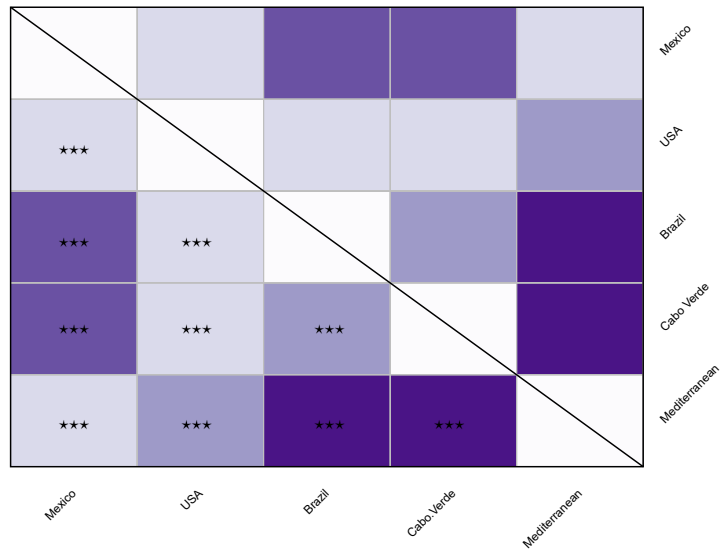
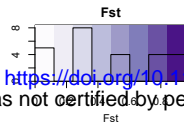


# Scenario V <sup>★</sup>

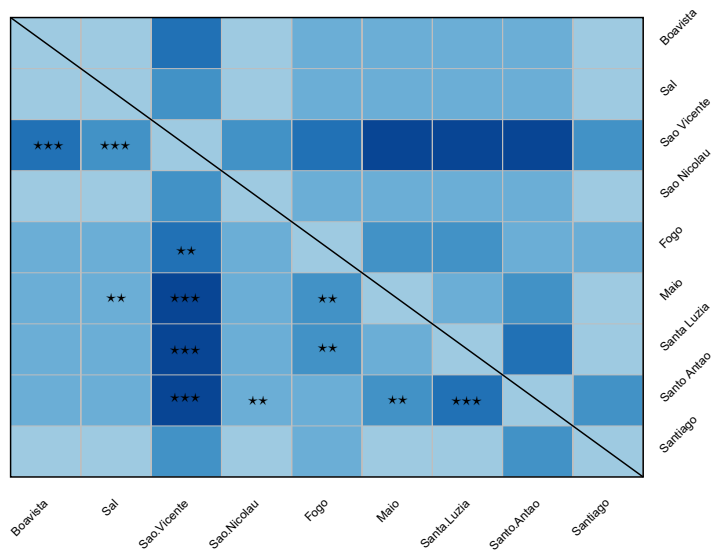
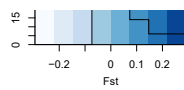


(a)

bioRxiv preprint doi: <https://doi.org/10.1101/2020.01.23.916866>; this version posted January 26, 2020. The copyright holder for this preprint (which was not certified by peer review) is the author/funder. All rights reserved. No reuse allowed without permission.



(b)



(c)

